

EVOLUTION OF TYPE IA SUPERNOVAE ON COSMOLOGICAL TIME SCALES

INMA DOMÍNGUEZ¹, PETER HÖFLICH², OSCAR STRANIERO³, CRAIG WHEELER²

¹*University of Granada, Granada, Spain*

²*University of Texas, Austin, USA*

³*Osservatorio Astronomico di Collurania, Teramo, Italy*

ABSTRACT. Due to their high luminosity at maximum and degree of homogeneity, Type Ia supernovae have been extensively used for cosmological purposes, in particular to estimate extragalactic distances and the Hubble constant. Recently the number of Type Ia supernovae detected at high redshift has increased, opening the possibility of determining the mass density parameter, the cosmological constant and the deceleration parameter. The observed supernovae appear to be further than expected -even for an empty Universe-, implying a low density Universe and moreover an accelerating Universe. Among the various uncertainties, we address the possibility that old supernovae are not equal to current supernovae. From first principles, an evolution of progenitors with time is expected. Additionally, some observations show a dependence of the observed properties on galaxy type and colour. Our aim in this work is to study the outcome of exploding CO white dwarfs following the evolution of the progenitor intermediate mass stars with different masses and metallicities. Once this influence of the progenitor has been determined, the observations may be corrected. At the present stage of this project we are not able to quantify this effect properly. One result is clear, that the differences at maximum are expected to be small (~ 0.2 mag) but this is of the same order as all the evidence for a positive cosmological constant (~ 0.25 mag).

1. Introduction

Type Ia supernovae are among the best candidates for cosmological research: they reach a luminosity of the same order as that of their host galaxies, a million times greater than Cepheids. Moreover, they are easier to understand than galaxies, because they are the explosion of a single object. For galaxies, it has been found that the variations with redshift are mainly due to their own evolution and not to cosmological effects (Tinsley, 1972; Oke, Gunn and Hoessel 1996). Concerning the used of SNIa as standard candles, the homogeneity of the SN event, or at least of their maximum luminosity at maximum, is a fundamental requirement. In this context, a relation between the maximum luminosity and another observable property is very usefull.

Supernovae are not equal; the variation of the luminosity at maximum is ~ 2 mag in B and ~ 1 mag in V, which is probably an indication of a different progenitor population. It has been shown that just excluding the redder events, by selecting those with B-V at maximum smaller than 0.5, reduces the dispersion in the Hubble diagram to values around $\sigma \sim 0.25$ (Hamuy et al. 1996b; Riess et al. 1996). Recently this dispersion was further reduced to $\sigma \sim 0.11$, using the maximum-decline relation (decline rate

from maximum during the first 15 days in the B band) and the multicolour light-curve shape (MLCS) methods to determine the maximum luminosity (see Phillips et al., 1993; Hamuy et al., 1996a and Riess et al., 1996). These methods provide a local calibration of the absolute luminosity, which is used at high redshift to infer the maximum luminosity. To do this, the SNe at high z are assumed to be equal to the local ones. The validity of this assumption is one of our concerns.

The use of the *maximum luminosity decline relation* to estimate the maximum luminosity of *normal* SNIa at $z \leq 0.1$ and the determination of the distance to host galaxies, using Cepheids observed by Hipparcos, have led to the successful determination of H_o . In addition, the linearity of the Hubble flow has been confirmed. At present, only small discrepancies related to the absolute calibration remain, a conservative estimate gives $H_o=60 \pm 10$ km/s/Mpc, in which the lower values, $H_o=56 \pm 5$ km/s/Mpc, are *preferred* (see Branch 1998 and references therein).

These discrepancies in the absolute distances do not affect the use of the high redshift supernovae for the determination of the cosmological parameters, because in this case just relative luminosity distances are employed.

The high redshift supernovae are further than expected, even for an empty Universe (Filippenko and Riess 1998; Schmidt et al. 1998). The luminosity distance depends on the different cosmological parameters (Ω_m , Ω_λ and Ω_k) in a different way. Therefore with sufficient observed supernovae at large redshifts it is possible to determine these parameters individually. The fluctuations in the Cosmic Microwave Background radiation (CMB) give limits in the Ω_m - Ω_λ plane orthogonal to those given by the high redshift supernovae. A very important result is that the CMB observations exclude the only value of Ω_m that is compatible with $\Omega_\lambda=0$ in agreement with the observations of high redshift supernovae (Hancock et al. 1998). These results are consistent with those obtained from the observations of the Mass/Luminosity ratio of galaxies; to date 1150 objects have been observed up to $z=0.6$, which give $\Omega_m=0.19 \pm 0.06$ (Carlberg et al. 1997). Other methods, like the variation of the number density of galactic clusters with redshift, are consistent with a value of $\Omega_m=0.3-0.34$ (Bahcall et al. 1997). Taking into account all these determinations, $\Omega_\lambda=0.62 \pm 0.16$ and $\Omega_m=0.24 \pm 0.10$ (Lineweaver, 1998). The observed number of gravitational lenses required $\Omega_\lambda \leq 0.7$ (Falco et al. 1998) for a flat Universe, which is consistent with the proposed values and should not be overlooked. The formation of large scale structures also depends on Ω_m . The *sponge like* observed structures would be already formed at $z = 2$, if Ω_m were ≤ 0.3 , while for $\Omega_m=1$ the formation would continue at the present time. From the high resolution spectra of distant quasars it is possible to infer the large scale structures, fitting the Lyman- α forest. In this case, one of the possibilities is a closed Universe with just pure baryonic matter and high Ω_λ , 1.07. Other possibilities agree with the above mentioned values for Ω_λ and Ω_m (van de Bruck and Priest 1998). In summary, all the above mentioned results favour a low density Universe with a positive cosmological constant.

1.1. Observed population age dependence

There exists observational evidence suggesting a dependence of the observed properties of SNIa on galaxy type and colour (see Hamuy et al. 1996a, Branch et al. 1996; Capellaro

et al. 1997; Wang et al. 1997). The SNe rate in spirals is double than in ellipticals and in spirals the SNe rate in the bulge decreases. The observed scatter in the SNIa light curves in ellipticals is smaller than in spirals and the SNe observed in ellipticals are less luminous in average than those observed in spirals ($\sim 0.3 \pm 0.1$ mag in B and V), with magnitudes similar to those occurring in the outer parts of spirals. The dispersion in the decay rate of the light curve and in the expansion velocities is greater in spirals.

This may indicate a variety in the progenitor population, which would probably be found on changing the redshift. If this is the case, the use of the luminosity decline relation or the MLCS method obtained for local SNe may lead to wrong results at high z . However, these local calibrations are made without taking into account properties of the host galaxy or of the site within the galaxy. This may imply that differences due to different progenitor populations have already been taken into account in these calibrations.

1.2. Evolutionary Effect

More massive progenitors evolve faster, which affects both the stars in the progenitor binary system and the binary parameters (distances, radii, conditions for mass overflow and the like). A similar situation occurs for lower metallicities, whereby low metal stars evolve faster and moreover have smaller radii. In the case of high redshift, we expect a major contribution of massive and low metallicity stars. This would change the characteristics of the binary systems and the relative contribution of the different scenarios to the SNIa population.

An additional consideration is that the properties of the interstellar medium are also expected to change. For example, current main contributors such as low mass red giants would not be present at large redshifts. The extinction law in the LMC and SMC is significantly different from that of the Milky Way (Bouchet et al. 1985). Moreover, the extinction law also depends on the redshift of the absorbing dust cloud (Höflich and Khokhlov, 1996). Therefore, if the extinction to local or far SNIa is significant, its dependence on metallicity should be taken into account.

2. Influence of the Initial Composition of the Exploding White Dwarf

Type Ia supernovae occur in all types of galaxies, including ellipticals, in which star formation ended some Gyr ago. This implies that a binary system is required as the progenitor of a Type Ia supernova because the stars currently evolving in such galaxies are low mass stars, which when evolving as single stars cannot explode.

As it is *well* known, the system that satisfactorily meet all the observational constraints for Type Ia supernovae is the thermonuclear explosion of an accreting CO white dwarf (Hoyle and Fowler 1960; for theoretical details see Wheeler and Harkness (1990), Woosley and Weaver (1994), Bravo et al. (1993 and 1996), Höflich and Khokhlov (1996), Nomoto et al. (1997). Three different candidates may reach this situation: the explosion of a CO white dwarf that reaches the Chandrasekhar mass by accretion from a MS or RG star, called the single degenerate Chandrasekhar mass scenario (Nomoto and Sugimoto, 1977; Nomoto, 1982); the explosion of a sub-Chandrasekhar mass CO

white dwarf that ignites He explosively in the outer layers, called the double detonation sub-Chandrasekhar mass scenario (Nomoto 1980, Limongi and Tornambé 1991; Woosley and Weaver, 1994, Höflich and Khokhlov, 1996); the explosion of a CO white dwarf that reaches the Chandrasekhar mass by merging with another CO white dwarf, called the double degenerate scenario (Iben and Tutukov, 1984).

None of these scenarios are completely satisfactory, because some fundamental problem is encountered in each of them. For the single degenerate Chandrasekhar mass it is the problem posed by Cassisi, Iben and Tornambé (1997; see also Tornambé and Pieranti in this volume) of the impossibility of growing by accretion of H to more than $\sim 1.1M_{\odot}$; consequently the Chandrasekhar mass cannot be attained. Additionally, the lack of H and He in the spectra and of radio emission means that the existence of the companion remains unproven. Sub-Chandrasekhar mass models cannot account for the observational properties of the majority of Type Ia supernovae (Höflich et al. 1997, Nugget et al. 1997). In the case of the double degenerate scenario, the question is that WD binaries with the proper masses are not observed at all, although several surveys have been carried out. Moreover, SPH simulations (Benz et al. 1990; Rasio and Shapiro 1995; Mochkovitch et al. 1997) do not produce a supernova in this way satisfactorily.

Table 1 - Delayed Detonation Models

	ρ_{tr} (10^7 g/cm 3)	Z^h/Z_{\odot}	C/O	E_{kin} (10^{51} erg/g)	M_{Ni} (M_{\odot})
DD21c	2.7	1.0	1.0	1.32	0.69
DD23c	2.7	1.0	2/3	1.18	0.59
DD24c	2.7	1/3	1.0	1.32	0.70
DD13c	3.0	1.0	1.0	1.36	0.79

On the other hand, all the above mentioned problems are relative. The question of whether or not the Chandrasekhar mass is achieved remains open; high accretion rates have been employed by several authors to achieve this and the observed counterparts may have been identified as super soft X ray sources, SSXRS (van den Heuvel et al. 1994, Rappaport et al. 1994a and 1994b). The sub-Chandrasekhar candidates have *normal* progenitors, which may explain some events (subluminous and blue). The most intriguing question now is probably why we do not observe them or why they do not occur. The double degenerate scenario lacks an observer counterpart: appropriate double white dwarf systems have not yet been observed, but these negative observational results maybe consistent with the expected numbers (Isern et al. 1997).

The three scenarios may occur and all of them may contribute to some extent to the Type Ia supernovae population. In the present study we choose the *single degenerate* M_{Ch} scenario and, for the description of the burning front, the delayed detonation explosion model (a deflagration that turns into a detonation in the outer layers; see Khokhlov 1991). Detonation, deflagration or delayed detonation may occur. We perform our study for the delayed detonation models, as these models give the best fit to the observations. Höflich and Khokhlov (1996) satisfactorily explained the observations

(light curves and spectra) of 27 Type Ia Supernovae within the delayed detonation (or its variation, pulsation delayed detonation) explosion of Chandrasekhar mass CO white dwarfs. For the delayed detonation models two parameters apply to the description of the velocity of the burning front: the ratio of the deflagration velocity to the local speed of sound and the transition density (the density at which the deflagration turns into a detonation).

In order to obtain a first estimate of the possible influence of the progenitors on the observed properties, Höflich, Wheeler and Thielemann (1998) recently studied the outcome (nucleosynthesis, light curves and spectra) of a set of CO white dwarfs in which the amount of C/O and the abundances of heavy elements (heavier than Ca) are parametrized (Z^h) (see Table 1). For the WD, the total mass ($1.4M_{\odot}$) and central density ($9 \cdot 10^9 \text{ g/cm}^3$) are fixed. For the description of the burning front, the ratio of the deflagration velocity to the speed of sound adopted is 0.03 and, except in one case, the transition density is $2.7 \cdot 10^7 \text{ g/cm}^3$. The values adopted are those that best reproduce the observed properties (light curves and spectra) of the majority of Type Ia supernovae.

This section summarises the results of these calculations, see Höflich, Wheeler and Thielemann (1998) for details. As shown in Table 1, decreasing the amount of C (the fuel) decreases the kinetic energy (column 5) and the amount of radioactive Ni (column 6), compare DD21c with DD23c. The Ni reduction is similar to the effect of decreasing the transition density (compare DD13c with DD21c). In this case, moreover, the kinetic energy is smaller, but not as much as in the previous case. In both, the chemical elements are more confined in velocity space and the region dominated by Si is narrower. This is due to the fact that when the kinetic energy is smaller, the outer layers have more time to expand, as in the case of a lower transition density. When the *metallicity* (elements heavier than Ca) is reduced, the changes in the amount of Ni and in the kinetic energy are small (compare DD21c with DD24c) and only a slightly larger amount of Ni is obtained.

When the amount of C is reduced, the luminosity at maximum is slightly greater ($\sim 0.08 \text{ mag}$). This is due to the fact that when the kinetic energy is smaller, less adiabatic cooling occurs and more of the stored energy contributes to the luminosity. On the other hand, the tail luminosity is smaller, as in this epoch the luminosity directly reflects the deposition of radioactive energy and the amount of Co is smaller. Therefore the light curve decline rate after maximum is steeper. This means that if the local relation is used to infer the luminosity at maximum, this luminosity would be underestimated ($\sim 0.1\text{--}0.3 \text{ mag}$), giving a wrong luminosity distance.

The change in *metallicity* (DD24c) influences the spectra indirectly. For lower metallicities, the amount of free electrons per nucleon, Y_e , is smaller implying a lower abundance of ^{54}Fe , which is an important source for the opacity in the UV region. The spectra is modified for $\lambda \leq 4000 \text{ \AA}$ and this influences the colours at different redshifts when this modification is shifted into different bands. The uncertainties at redshifts $z \geq 0.2$ in $\Delta(B - V)$ are of ~ 0.3 . Nonetheless, these modifications affect the regions with velocities of 10000–12000 km/s that have been subjected to oxygen burning and are seen around maximum. Later on, the observed light comes from the inner layers which have been subjected to explosive burning and therefore Y_e and the abundances of the neutronised elements are determined by the electron captures and do not depend on the initial

composition of the WD.

3. Evolution of Intermediate Mass Stars: the CO Core

All the proposed progenitors for Type Ia supernovae rely on the explosion of a CO white dwarf. The mass of the accreting CO white dwarf and its chemical composition influence the pre-explosion evolution and the explosion itself (energy and nucleosynthesis) and consequently the observational properties.

CO white dwarfs are initially the degenerate CO cores of intermediate mass stars and their mass and chemical composition depend on the evolutionary history of the progenitor star. The FRANEC (Frascati RAphson Newton Evolutionary Code) has been used for all the evolutionary models computed in this work. See Straniero, Chieffi and Limongi (1997) and Chieffi, Limongi and Straniero (1998) for a full description of the code.

More massive stars have more massive CO cores, while higher metallicities (provided $Z \geq 10^{-6}$) mean less massive cores. When the CO core formed is greater than $\sim 1.1 M_{\odot}$, C is ignited and burns to O and Ne. The maximum mass for which C is not ignited, the so-called M_{up} , depends on the initial composition. This decreases with decreasing metallicity, to a certain value ($Z \sim 10^{-6}$, see Tornambé and Chieffi, 1986). We obtained $M_{up} = 8M_{\odot}$ for $Z=0.02$ and $6.5M_{\odot}$ for $Z=0.0001$; The final CO core mass and composition are determined by the evolutionary history, for which the treatment of turbulent convection, nuclear reaction rates, the equation of state and opacities are crucial (see Domínguez et al. 1998).

Once the central He is exhausted, the star enters the Asymptotic Giant Branch phase (AGB), usually divided into the early AGB (E-AGB) and the Thermal Pulse AGB phases (TP-AGB). The E-AGB is characterized by the establishment of the He burning within a shell outside the contracting CO core. Such an occurrence has two important effects in the evolution of the star: the CO core grows with time and the energy generated by the He shell expands the outer layers and cools the H burning shell, which is spent or nearly spent. At this moment the convective envelope can penetrate inward, pushing protons towards the vicinity of the He burning shell where, due to the high temperatures, the H is reignited and the thermal pulses (TP-AGB) begin. During this phase the recursive re-ignition of the H and He burning shells implies a further increase of the CO core mass. However it is believed that the strong AGB mass loss could prevent the occurrence of a large number of thermal pulses. Notice that without this mass loss, the CO core size could attain the Chandrasekhar mass. However, the observed maximum luminosity of the AGB stars in our galaxy and in the Magallanic clouds (Weidemann 1987; Wood et al. 1992) and the high mass loss rates observed at the tip of the AGB indicate that the envelope is lost and few pulses have time to occur. Therefore the mass of the CO white dwarf is essentially determined by the value reached at the end of the E-AGB phase (Vassiliadis and Wood, 1993).

For the bigger masses ($M \geq 5M_{\odot}$, for $Z=0.02$ or $M \geq 4M_{\odot}$ for $Z=0.0001$) the H shell is completely extinguished and the inward penetration of the convective envelope enters the He core, which is called the 2nd dredge up.

3.1. CO core mass

If we compare the results of different stellar evolutionary codes, differences of up to 50% in central He burning life times are found (see Domínguez et al. 1998). The longer the central helium burning life time, the greater is the time in which the H shell advance in mass and the increment of the He core mass will be greater. The convective algorithm is important; for example, if we compare the central He burning time in two models, one without overshooting, semiconvection or breathing pulses and the other, like ours, with just semiconvection, the He burning life time is double in the second case. To decide between different mixing hypotheses, the RGB, HB and AGB theoretical life time ratios are compared to the observed stellar number ratios of well studied galactic globular clusters (see Renzini and Fusi Pecci, 1988). The semiconvection scheme satisfactorily reproduces the observations but a moderate amount of mechanical overshooting cannot be ruled out.

The current uncertainty about the rate of the $^{12}\text{C}(\alpha, \gamma)^{16}\text{O}$ reaction introduces an additional problem. The larger the reaction rate, the longer the He burning life time. More quantitatively, the He burning life time could change by 5–10%. For the bigger masses, a different phenomenon will contribute to determine the final CO core mass. In fact, in such a star, the growth of the CO core at the end of the E-AGB is frozen by the occurrence of the 2nd dredge-up. Again the treatment of convective instabilities is crucial.

Table 2 - Properties of the CO core during the TP-AGB phase

M_T	Z	Y	M_{CO}	C_C	C/O_{core}	C/O_{Mch}	Rate	TP (number)
1.5	0.001	0.23	0.560	0.260	0.533	0.781	CF85	3
3.0	0.001	0.23	0.738	0.289	0.610	0.772	CF85	2
5.0	0.001	0.23	0.907	0.316	0.563	0.691	CF85	1
6.0	0.001	0.23	0.976	0.320	0.537	0.650	CF85	1
3.0	0.0001	0.23	0.791	0.286	0.587	0.741	CF85	1
3.0	0.001	0.28	0.815	0.297	0.623	0.760	CF85	8
3.0	0.02	0.28	0.561	0.232	0.522	0.778	CF85	3
3.0	0.001	0.23	0.750	0.279	0.570	0.742	B-H96	6
3.0	0.001	0.23	0.727	0.654	2.314	1.525	B-L96	5
3.0	0.001	0.23	0.759	0.289	0.621	0.773	CF85	11

3.2. C/O gradient

The C/O gradient within the core is *built* in successive phases with different characteristics: convective central He burning (HB), radiative shell He burning during the early AGB phase and *rapid* convective shell He burning during the TP-AGB phase. Once enough He is depleted and C formed, the burning also occurs through the $^{12}\text{C}(\alpha, \gamma)^{16}\text{O}$ reaction. For higher temperatures, the 3α reaction dominates. This is the reason why the central C is greater for more massive stars, in which less C is destroyed by the $^{12}\text{C}-\alpha$

capture. Just outside the convective He burning core, an instability develops due to the chemical gradient, called semiconvection. Note that, in some way a small amount of convective core overshoot mimics the global effect of semiconvection. Toward the end of the central He burning, when the He mass fraction in the convective core is reduced to 0.1, the occurrence of breathing pulses (Castellani et al. 1985) could delay the He exhaustion. This allows more time for the $^{12}\text{C}-\alpha$ capture reaction to act and significantly less C is obtained, while the final CO core is slightly bigger. In our code these pulses are inhibited, taking into account observational constraints (Caputo et al. 1989).

The temperature of the He burning shell is higher than that of the central He burning. Nonetheless, more C is left by the shell burning than by the central C burning. This is due to the rapid advance of the shell, as the $^{12}\text{C}-\alpha$ does not have much time to convert C into O. As the burning is radiative, a pronounced C gradient is *built* during the E-AGB. This gradient is steeper for the smaller masses of our interval. The temperature in the convective burning He shell during the TP phase is higher but these pulses are very rapid and the C is not burnt, so that a $\text{C}/\text{O} \geq 1$ is obtained. However, it is believed, as explained in the introduction, that few pulses occur. Therefore the contribution of the TP phase to the CO core mass and composition is not significant. The carbon abundance gradient within the CO core for the $3M_{\odot}$ ($Z=0.001$; $Y=0.23$) model is shown in Figure 1. The final average C abundance within the CO core (see column 6, $\text{C}/\text{O}_{\text{core}}$, Table 2) decreases for greater progenitor masses, from $3M_{\odot}$ to $6M_{\odot}$. The maximum difference obtained is of 13%. When metallicity is varied, a maximum difference in the C abundance of 17% is obtained. In both cases, the differences are smaller than those found in the parametrized models (Höflich, Wheeler and Thielemann, 1998).

For the accreted matter from the companion, a C/O abundance equal to 1 is assumed (Nomoto et al., 1984). This point is weak and critical, especially for the smaller masses of our interval for which the mass accreted to reach the Chandrasekhar mass is greater than the initial CO core mass. In fact, the average C abundance (see column 7, $\text{C}/\text{O}_{\text{Mch}}$, in Table 2) is finally larger in the $1.5M_{\odot}$ model than in the $3M_{\odot}$ model, due to this accreted *top*. However, this is probably the correct assumption. In fact, we know from AGB models that the C/O left by the thermally pulsing He shell, a situation that resembles the burning of He above the CO white dwarf, is just slightly greater than 1. When the average C abundance in the Chandrasekhar mass WD is considered, the differences between different progenitor masses are more pronounced, 18%, as the accreted matter is more significant for the smaller masses. On the other hand, when the same operation is performed for progenitors with different metallicities, the differences in C abundance tend to be eliminated as the amount of accreted matter is smaller for the models with lower metallicities for which the amount of C is bigger, until finally between the most extreme cases in metal content, the difference is reduced to 5%.

In summary, the phase of accretion onto the CO WD should be simulated in a more realistic way, as the chemical profile *acquired* during this phase has an important weight in the average C abundance. Moreover, the amount of C will influence not only the conditions at the ignition point but also the propagation of the burning front (see

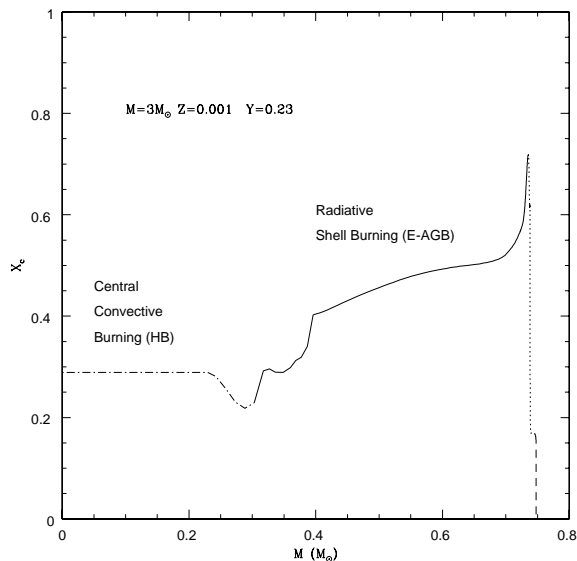


Fig. 1. Carbon abundance (mass fraction) at the beginning of the TP-AGB phase. The different evolutionary phases, HB, E-AGB and TP-AGB produce a different carbon abundance gradient.

Bravo et al. 1996). It will be very important to clarify whether it is possible to reach the Chandrasekhar mass by H accretion. If the answer is negative, the single degenerate Chandrasekhar mass scenario, in spite of all its advantages, should be abandoned and the merging of CO white dwarfs would remain as the only alternative. We are studying the possibility of constraining the scenario, taking into account the different C/O expected in the outer layers. For example, the double degenerate scenario would show a dependence on metallicity, while this dependence would not appear in the single degenerate scenario.

It is obvious that the rate adopted for the $^{12}\text{C}(\alpha, \gamma)^{16}\text{O}$ is very important. By Taking the high and low rates obtained by Buchmann (1996, 1997), the average C/O abundance within the CO core is 4 times greater for the lower rate (see models B-H96 and B-L96 in Table 2). In the FRANEC code, the adopted rate is that of Caughlan and Fowler (1985, CF85 in Table 2) which is close to the high rate. The correct rate may be somewhere in between, so our C/O abundances within the CO core could be lower limits.

4. Conclusions

Going back in time, we expect a major contribution of massive and low metallicity stars. This would change the characteristics of systems with mass overflow (less metallicity means more compact stars with bigger CO cores) and the chemical C/O profile within the CO core. From our results, we expect, on average, less C for both more massive and low metal stars. The differences expected are smaller than 20%. When this is compared with the results of the parametrized models, a difference of ~ 0.2 mag is expected

for the inferred maximum luminosity. This is small but it is of the same order as the differences in maximum luminosity that allows us to discern the different values of the mass density parameter and the cosmological constant (~ 0.25 mag). Following our models, the maximum absolute magnitudes of high redshift supernovae are being underestimated, which would mean that these supernovae are even further. Nevertheless, it should be remembered that this result is just a first step and important points remain to be clarified. A critical factor is the composition adopted for the accreted matter. Open questions are the relations between progenitor mass and redshift and metallicity and redshift. The dependence of metallicity on redshift is highly uncertain. A detailed study of the host galaxies is needed but it is the situation when the progenitor was formed that is most relevant.

We are currently computing the outcome (explosions, light curves and spectra) of the models shown in Table 2. The influence of the C abundance gradient on the propagation of the burning front is an important issue. The amount of fuel, carbon, directly changes the energy of the explosion (both kinetic and radioactive energy) although a different parametrization of the burning front would have the same consequences. Metallicity may have an important effect on the explosion, although 1D explosion models limit our possibilities of taking this into account properly.

On examining the pre-supernova and supernova evolution, several uncertainties remain and for cosmology studies a difference of just 0.2 mag is significant.

The observations at high redshift show a very homogeneous event. *Why are they so homogeneous (or apparently so) when there are so many theoretical ways for them to vary ??*

References

- Bahcall N.A., Fan X., Cen R.: 1997, *Astrophys. J. Lett.* **485**, LL53
Benz W., Cameron A.G.W., Bowers R.L., Press WH: 1990 *Astrophys. J.* **348**, 647
Bouchet P., Lequeux J., Maurice, E., Prevot, L., Prevot-Burnichon, M.L.: 1985, *Astron. Astrophys.* **149**, 330
Branch D., Romanishin W., Baron E.: 1996, *Astrophys. J.* **465**, 73;erratum 467 473
Branch D.: 1998, *Ann. Rev. Astron. Astrophys.* **36**, 17
Bravo E., Domínguez I., Isern J., Canal R., Höflich P.A., Labay J.: 1993 *Astron. Astrophys.* **269**, 187
Bravo E., Tornambé A., Domínguez I., Isern J.: 1996 *Astron. Astrophys.* **306**, 811
Buchmann L.: 1996, *Astrophys. J.* **468**, L127
Buchmann L.: 1997, *Astrophys. J.* **479**, L153
Capellaro et al.: 1997 \dot{A} 322 431
Caputo F., Castellani, V., Chieffi A., Pulone L., Tornambé: A. 1989 *Astrophys. J.* **340**, 241
Carlberg R.G., Yee H.K.C., Ellingson E.: 1997 *Astrophys. J.* **478**, 462
Cassisi S., Iben I., Tornambé A.: 1998 *Astrophys. J.* **496**, 376
Castellani V., Chieffi A., Pulone L., Tornamé: 1985 *Astrophys. J.* **296**, 204
Caughlan G.R , Fowler A.M.: 1985 *Ann. Rev. Astron. Astrophys.* **21**, 165
Chieffi A. and Straniero O.: 1989, *Astrophys. J.* **71**, 47

- Domínguez I., Höflich P., Wheeler J.C., Straniero O.: 1998, in preparation
- Domínguez I., Chieffi A., Limongi M., Straniero O.: 1999, submitted to ApJ
- Falco E.E., Kochanek C.S., Munoz J.A.: 1998 *Astrophys. J.* **494**, 47
- Hancock S., Rocha G., Lasenby A.N., Gutierrez C.M.: 1998 *Mon. Not. R. Astr. Soc.* **294**, L1
- Hamuy M., Phillips M.M., Schommer R.A., Suntzeff N.B., Maza J., Aviles A.: 1996a, *Astron. J.* **112**, 2391
- Hamuy M., Phillips M.M., Suntzeff N.B., Schommer R.A., Maza J., Aviles A.: 1996b, *Astron. J.* **112**, 2398
- Höflich, P. 1995: *Astrophys. J.* **443**, 89
- Höflich P., Wheeler J.C., Thielemann F.K 1998: *Astrophys. J.* **495**, 617
- Höflich P., Khokhlov A., Wheeler C.J., Nomoto K., Thielemann F.K.: 1997 in *Thermonuclear Supernovae*, Kluwer Academic Publisher
- Höflich P., Khokhlov A. 1996: *Astrophys. J.* **457**, 500
- Höflich P., Khokhlov A., Wheeler J.C.: 1995, *Astrophys. J.* **444**, 211
- Hoyle P., Fowler W.A.: 1960 *Astrophys. J.* **132**, 565
- Iben I.J Tutukov A.V.: 1984 *Astrophys. J. Suppl.* **54**, 335
- Isern J., Hernanz M., Salaris M., Bravo E., Garcia-Berro E., Tornambe A.: 1997 in *Thermonuclear Supernovae*, Kluwer Academic Publisher
- Khokhlov A.: 1991 *Astrophys. J.* **245**, 114
- Limongi M., Tornambé A. 1991 *Astrophys. J.* **371**, 317
- Lineweaver C.H., 1998 *Astrophys. J. Lett.* **505**, L69
- Mochkovitch R., Guerrero J., Segretain L.: 1997 in *Thermonuclear Supernovae*, Kluwer Academic Publisher
- Nomoto K., Sugimoto D.: 1977 *Publ. Astron. Soc. Japan* **29**, 765
- Nomoto K.: 1982 *Astrophys. J.* **253**, 798
- Nomoto K., Thielemann F.-K., Yokoi K. 1984, *Astrophys. J.* **286**, 644
- Nugent P., Baron E., Branch D., Fisher A. Hauschildt P.: 1997 *Astrophys. J.* **485**, 812
- Oke J.B. Hoessel J.E. Gunn J.G.: 1996 *Astron. J.* **111**, 29
- Perlmutter C. et al. 1995: *Astrophys. J. Lett.* **440**, L95
- Perlmutter C. et al. 1997: *Astrophys. J.* **483**, 565
- Rasio F.A. Shapiro S.L.: 1995 *Astrophys. J.* **438**, 887
- Rappaport, S., Chiang, E., Kallman, T. Malina, R.: 1994a, *Astrophys. J.* **431**, 297
- Rappaport, S. Di Stefano, R., Smith J.: 1994b *Astrophys. J.* **426**, 692
- Renzini A. Fusi Pecci F.: *Ann. Rev. Astron. Astrophys.* **26**, 199
- Riess A.G., Press W.H., Kirshner R.P.: 1995, *Astrophys. J.* **438**, L17
- Riess A.G., Press W.H., Kirshner R.P.: 1996, *Astrophys. J.* **473**, 88
- Riess A.G., et al.: 1998 *Astrophys. J.* **in**, press
- Straniero, O. Chieffi, A. and Limongi M.: 1997 *Astrophys. J.* **490**, 425
- Straniero, O. Chieffi, A., Limongi M. Dominguez, I.: 1998 in *Views on Distance Indicators*, *Mem. Soc. Astron. It.* **Ed.**, F.Caputo, in press
- Thielemann F.K., Nomoto K., Hashimoto M.: 1996, *Astrophys. J.* **460**, 408
- Tinsley, B.: 1972 *Astrophys. J.* **178**, 319
- Tornambé A. Chieffi. A.: *Mon. Not. R. Astr. Soc.* **1986**, 220,529
- van de Bruck C., Priester W.; 1998 astro-ph/9810340

van den Heuvel, E.P.J., Battacharya, D., Nomoto, K. Rappaport, S.: 1992, Å262 97
Wang L., Höflich P., Wheeler J.C., 1997, *Astrophys. J.* **483**, 29
Wheeler C.J., Harkness R.P.: 1990 Rep. Prog. Phys. 53, 1467
Wosley S.E., Weaver T.A.: 1986 *Ann. Rev. Astron. Astrophys.* **24**, 205
Wosley S.E., Weaver T.A.: 1994 *Astrophys. J.* **423**, 371